HST imaging and Morphology

Jeffrey Chan
and the GOGREEN collaboration

Summary of the HST imaging

1-orbit depth **WFC3/F160W** imaging for **12** of the GOGREEN clusters
1 x 2 rectangular tiling (136’’ x 233’’) = 24 orbits

Cluster	z	R200 (Mpc)	HST/FOV (out of x R200)
SPT-CL J2106	1.132	1.24	0.77
SpARCS J0335 (CDFS-41)	1.368	0.69	1.42
SpARCS J1634	1.177	0.86	1.12
SPT-CL J0205	1.320	0.66	1.48
SpARCS J0219 (XMM-67)	1.300	0.79	1.24
SpARCS J0035	1.335	0.93	1.05
SpARCS J1033	1.455	-	-
SpARCS J1638	1.196	0.70	1.38
SpARCS J1034	1.400	0.25	3.93
SpARCS J1051	1.035	0.92	1.92
SPT-CL J0546	1.067	1.23	0.77
SpARCS J1616	1.156	0.92	1.04

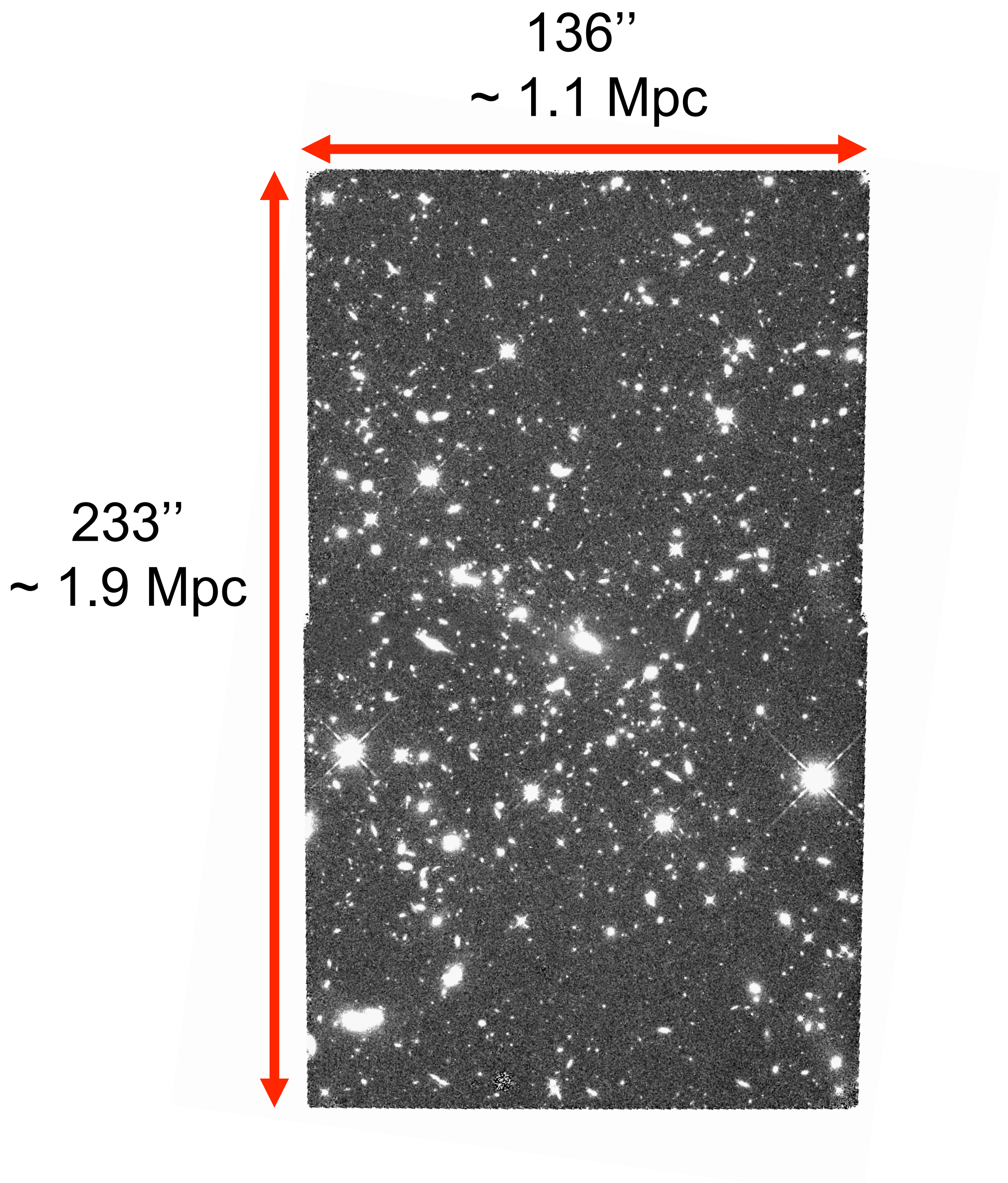

Summary of the HST imaging

1-orbit depth **WFC3/F160W** imaging for **12** of the GOGREEN clusters
1 x 2 rectangular tiling (136’’ x 233’’) = 24 orbits

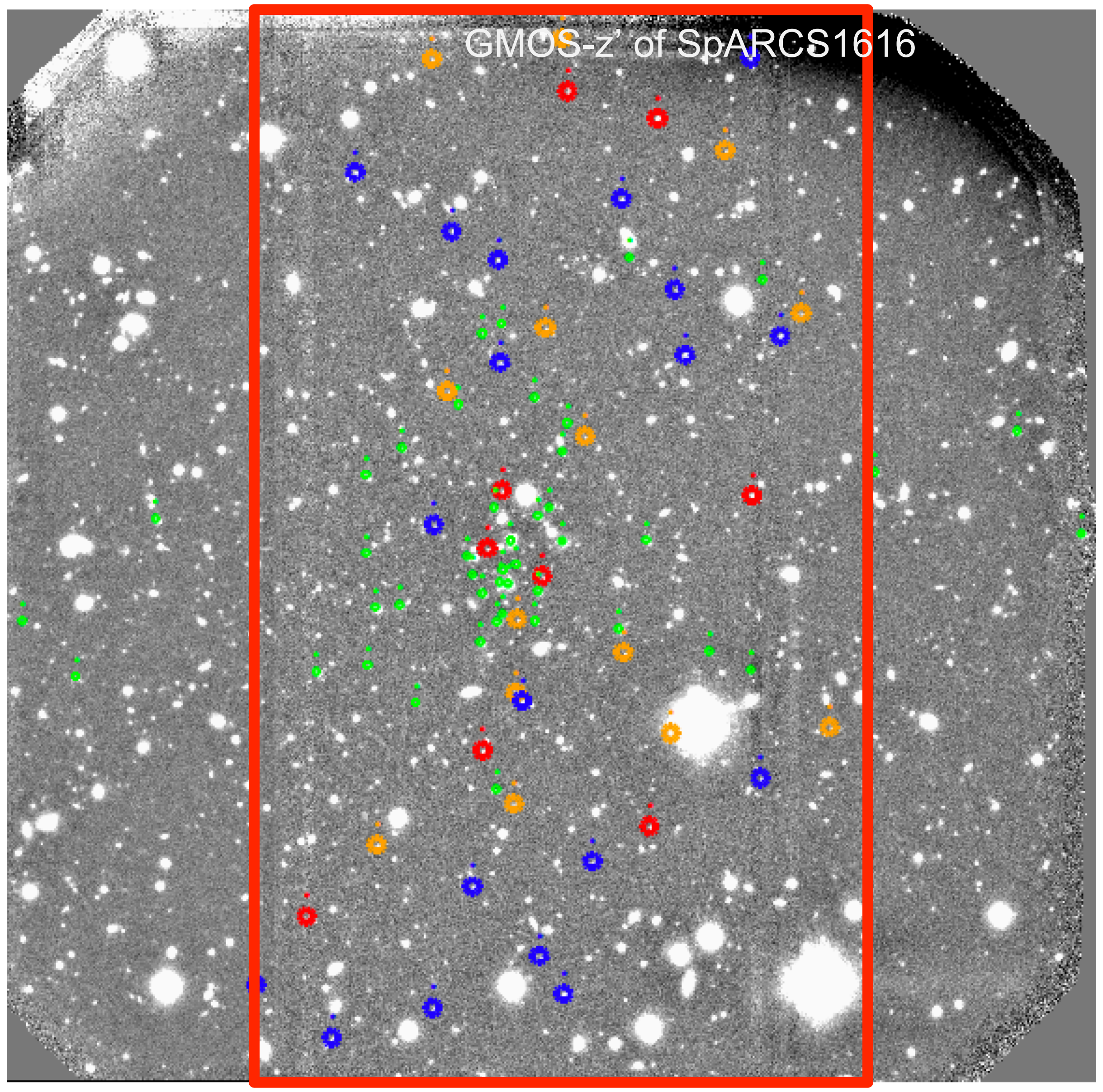

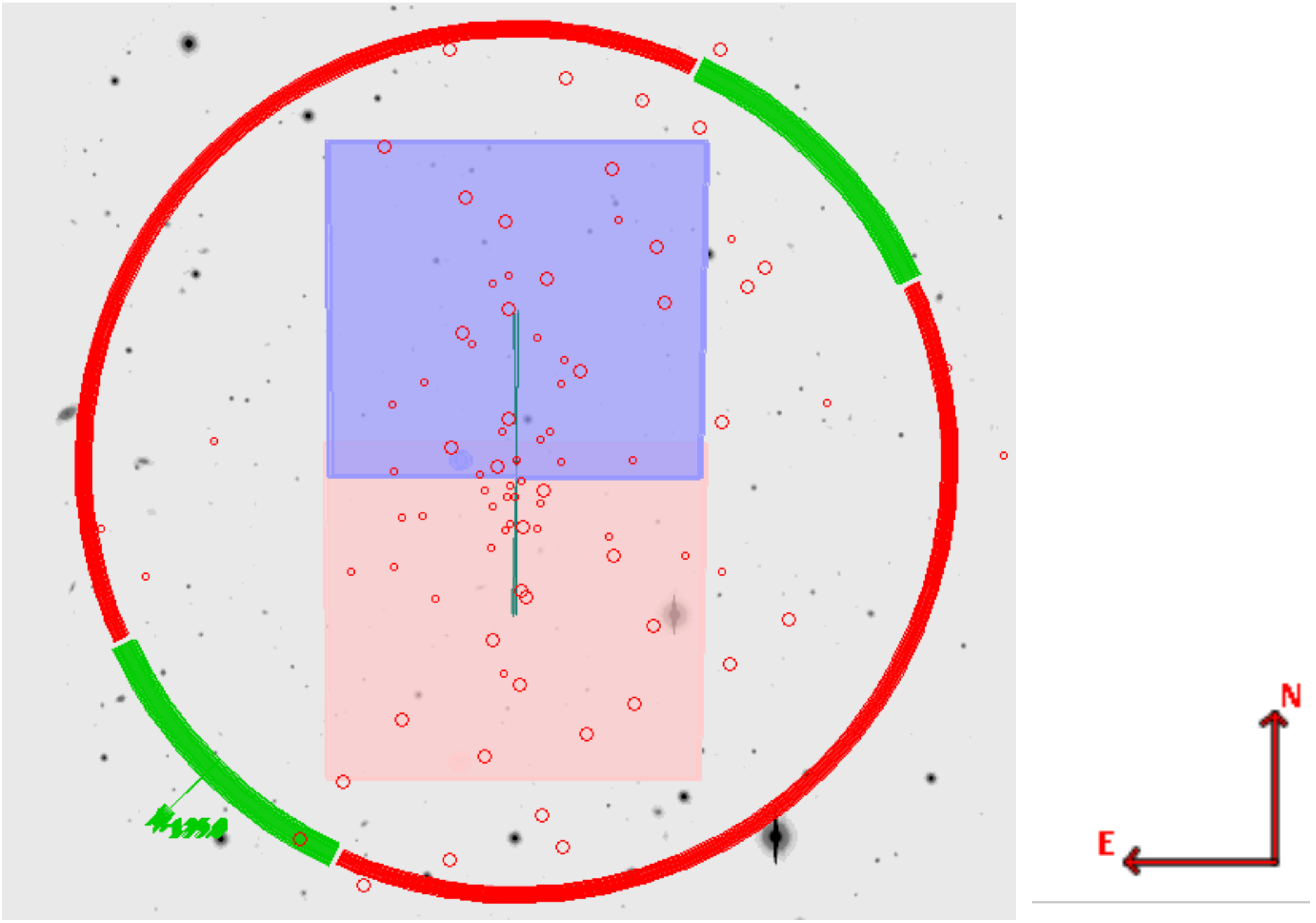

The tiling is oriented to the GMOS mask orientation to maximize the overlap between imaging and spectroscopy

Summary of the HST imaging

1-orbit depth **WFC3/F160W** imaging for **12** of the GOGREEN clusters
Reduced F160W images of the 12 clusters + archive HST imaging (red) are included in the release (data release content talk later this afternoon)

Cluster	z	Available Band
SPT-CL J2106	1.132	**ACS F606W, F814W (12477),** UVIS F814W, IR F105W/F140W (13677)
SpARCS J0335 (CDFS-41)	1.368	-
SpARCS J1634	1.177	**F140W (GCLASS)**
SPT-CL J0205	1.320	**ACS F606W, F814W (12477, 14677),** UVIS F814W, IR F105W, F140W (13677), F110W (14677)
SpARCS J0219 (XMM-67)	1.300	-
SpARCS J0035	1.335	UVIS F814W, IR F105W, F140W (13677, 14327) **F140W (GCLASS)**
SpARCS J1033	1.455	-
SpARCS J1638	1.196	**F140W (GCLASS)**
SpARCS J1034	1.400	-
SpARCS J1051	1.035	**F140W (GCLASS)**
SPT-CL J0546	1.067	**ACS F606W, F814W (12477)**
SpARCS J1616	1.156	**F140W (GCLASS)**

Structural parameters

Structural parameters derived from HST/WFC3 F160W imaging using Sersic fitting with GALAPAGOS v2.3.0 with galfitm-1.2.1
Single Sérsic fits (total mag, Sérsic index n (0<n<12) , Effective radius Re (0<Re<400pix), axis ratio q (0.0001<q<1), P.A.)

For H160 ~ 23.0 (logM~9.5):
Re: a bias of ~-6%, 1σ ~18%.
n: a bias of ~-13%, 1σ ~20%.
q: a bias of ~2%, 1σ ~6%.

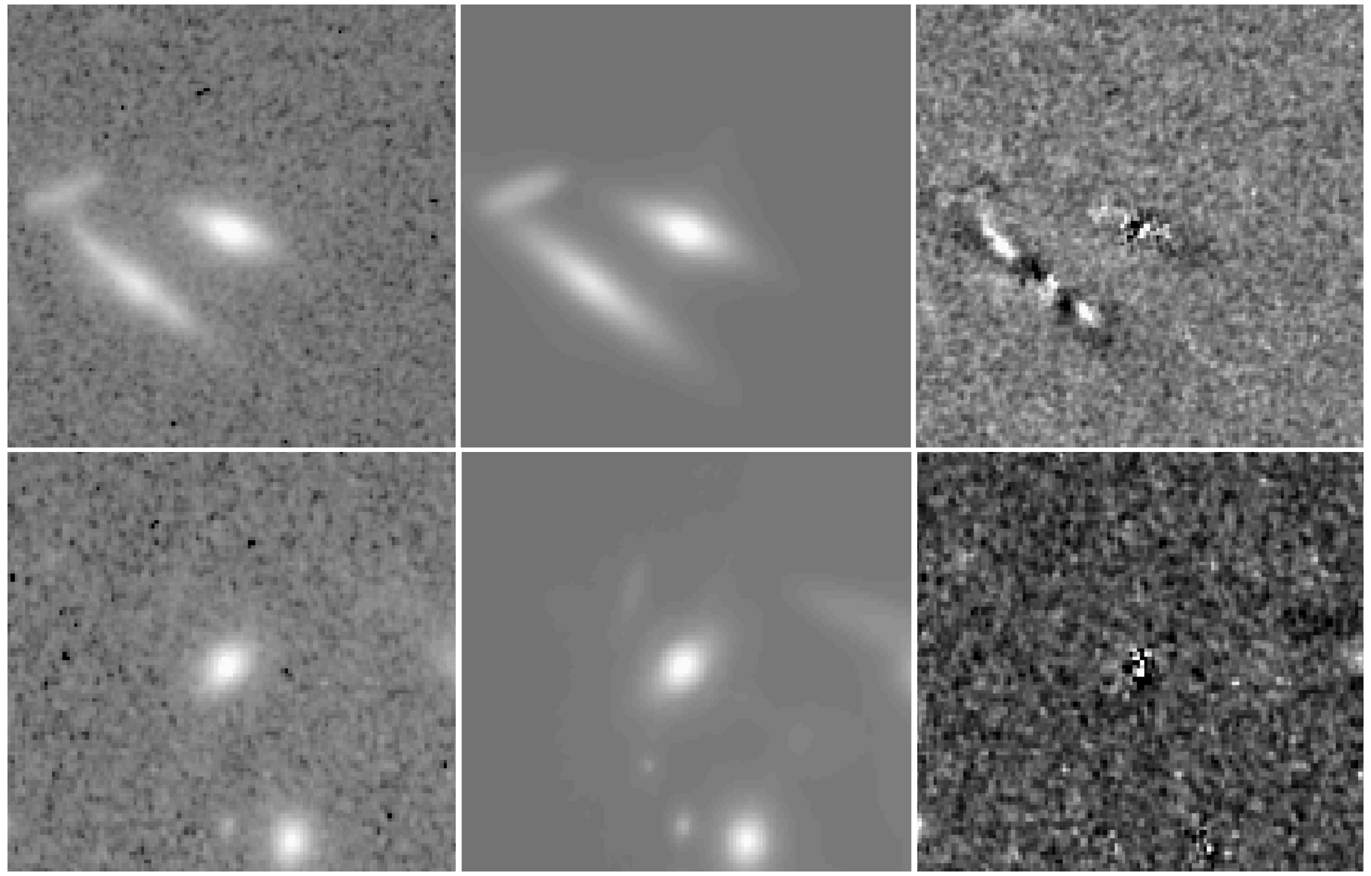

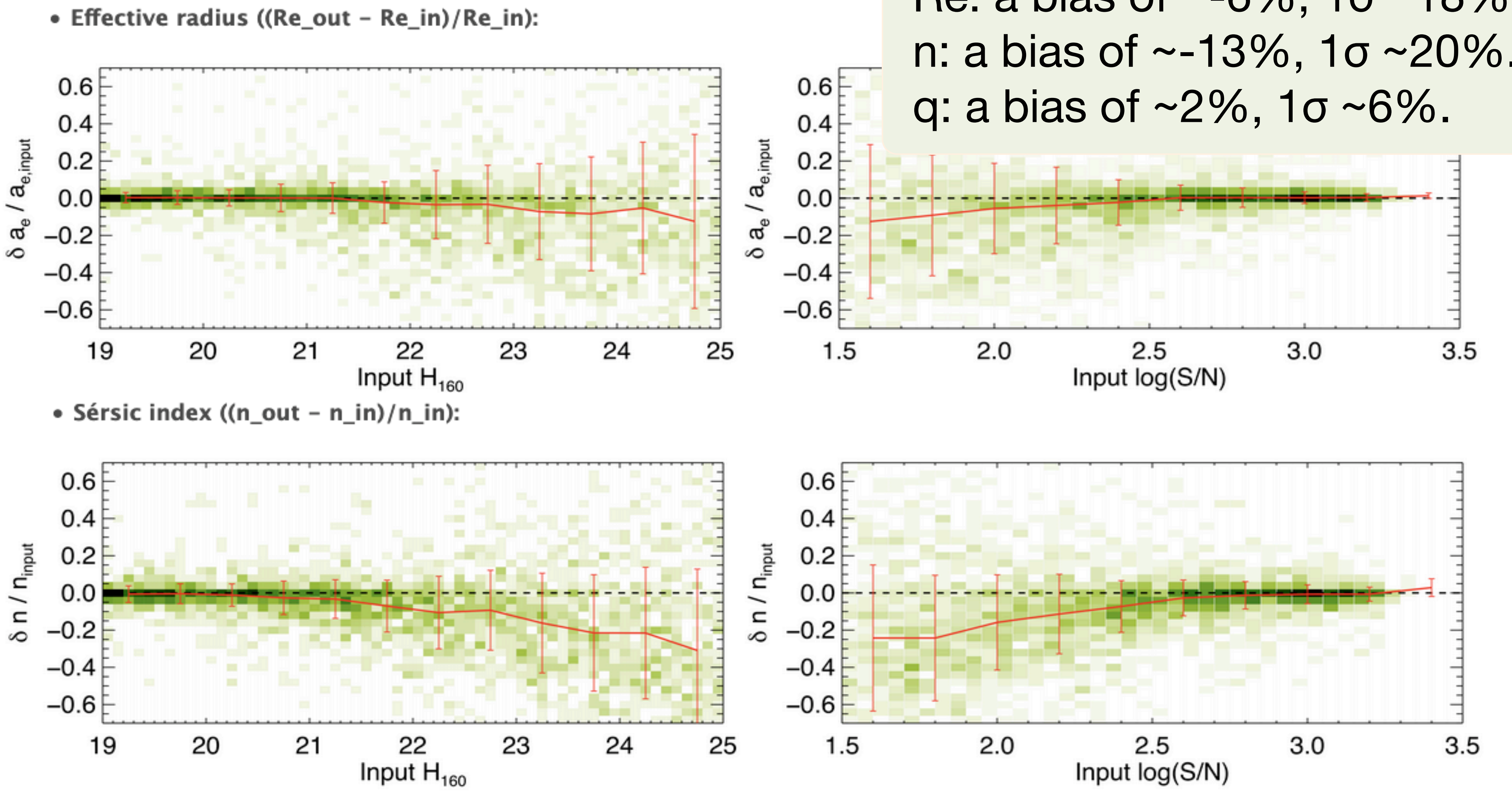

Morphologies of GOGREEN galaxies

- Goal: Compare the morphologies and structural properties between cluster and field galaxies to study the effect of environment on galaxy morphology at z>1

- Sample selection:
  z_{spec} & z_{phot} selected, down to logM~9.5

Cluster sample:
- 11 GOGREEN clusters (1.0 <z <1.4)
- **$N_{cluster}$: 832**

Field sample:
- CANDELS/3D-HST
- **$N_{CANDELS/3DHST}$: 6471**

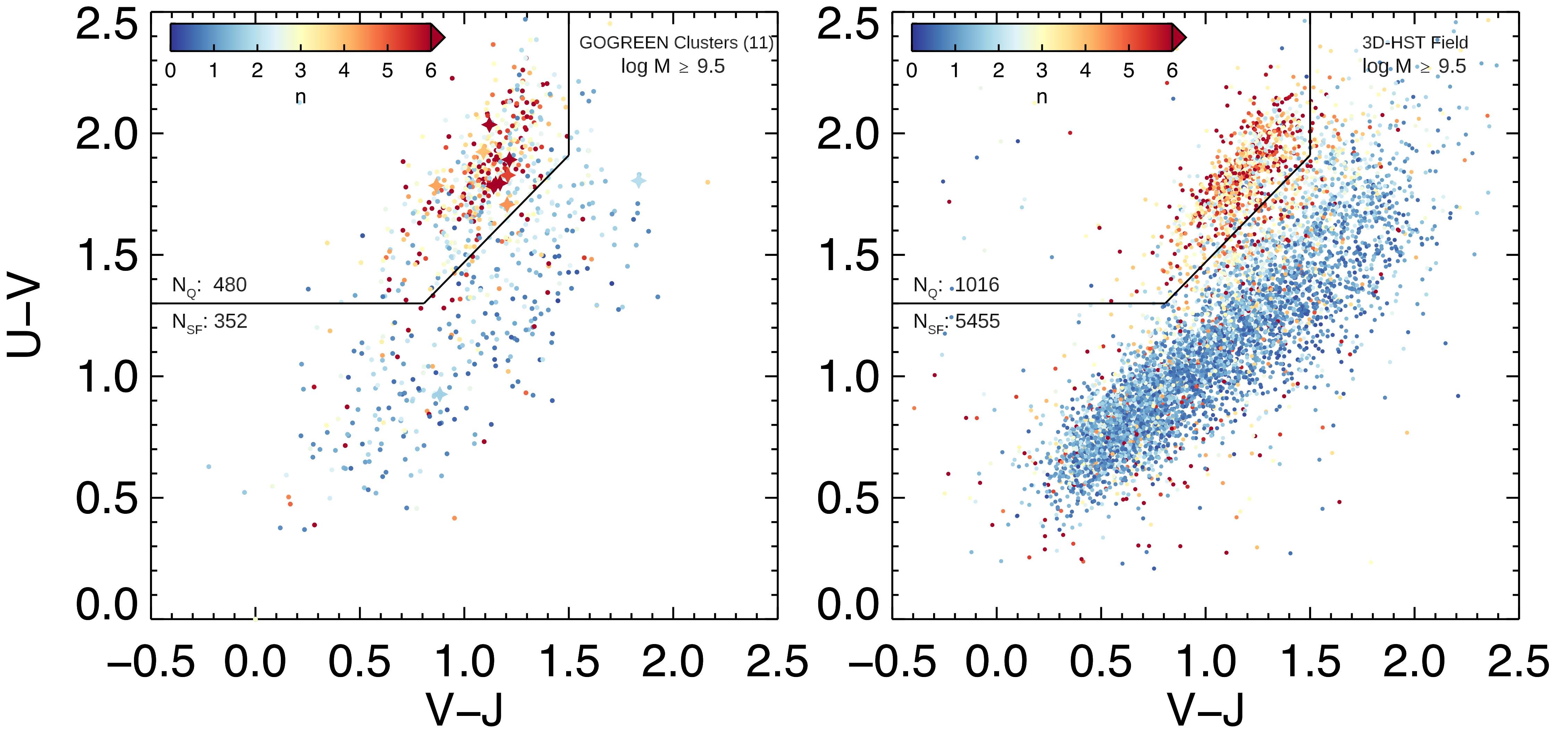

- Mass-size relations
- **Axis ratio distributions (Most accurate parameter! – Chan+20, in prep.)**
- Visual morphologies
- etc …

Ongoing work – Axis ratio distributions in clusters vs. field

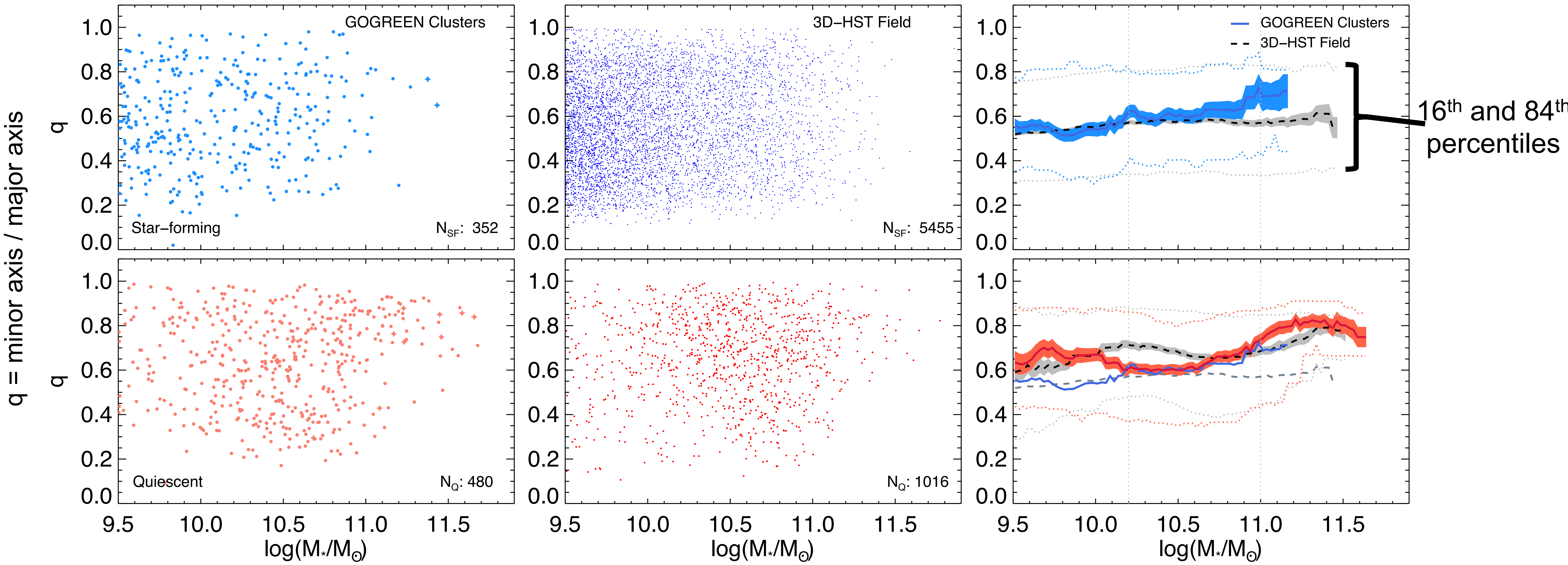

- Median *q* increases with mass for both SF and Q
- log(*M*) ≥ 11 Q galaxies are round and have narrower *q* distribution, similar to low-z
- Cluster vs. field differences: logM ~ 10.4 and logM ~ 11.1

Chan+20, in prep.

Cluster vs. Field – Axis ratio distributions

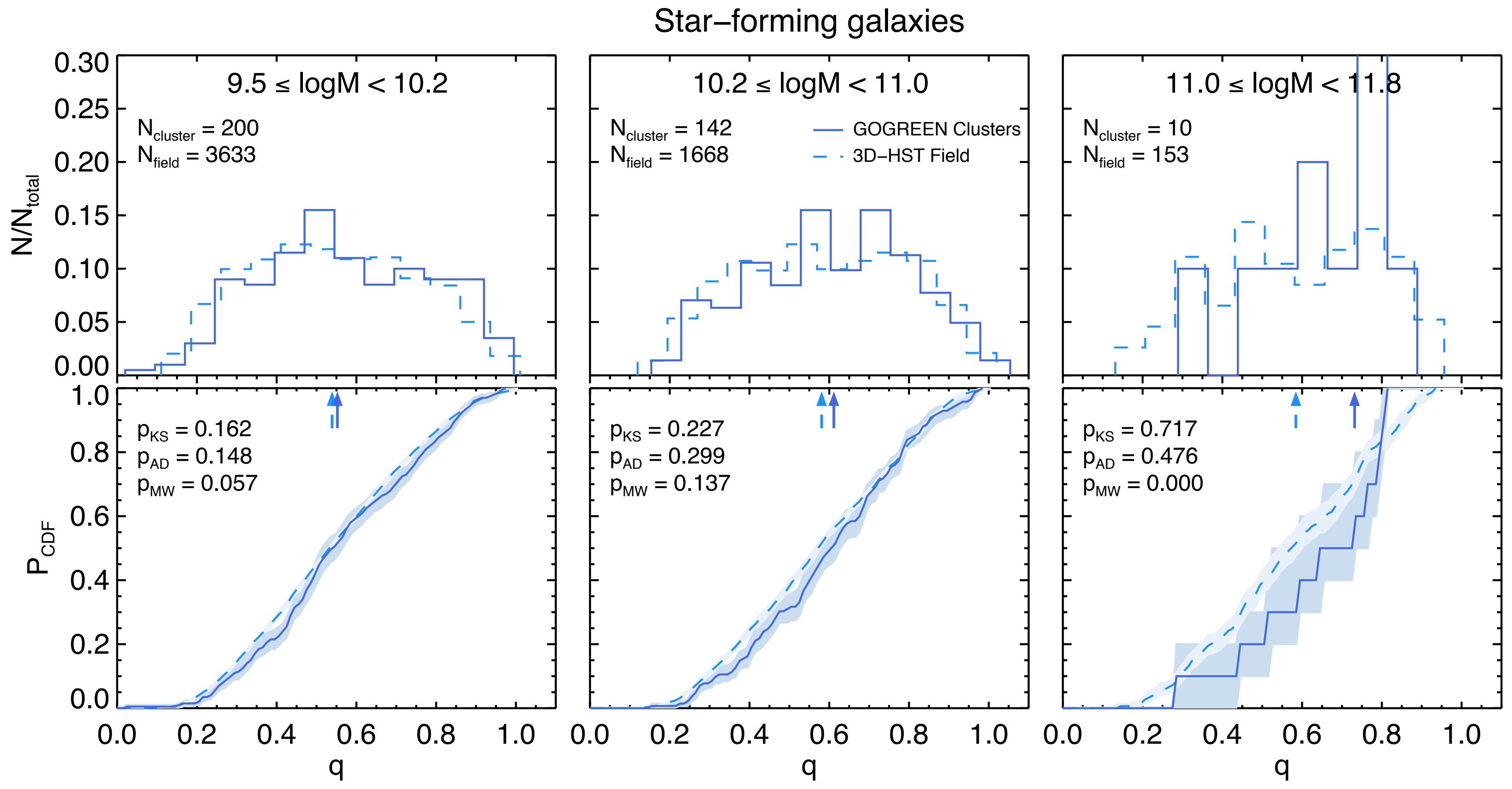

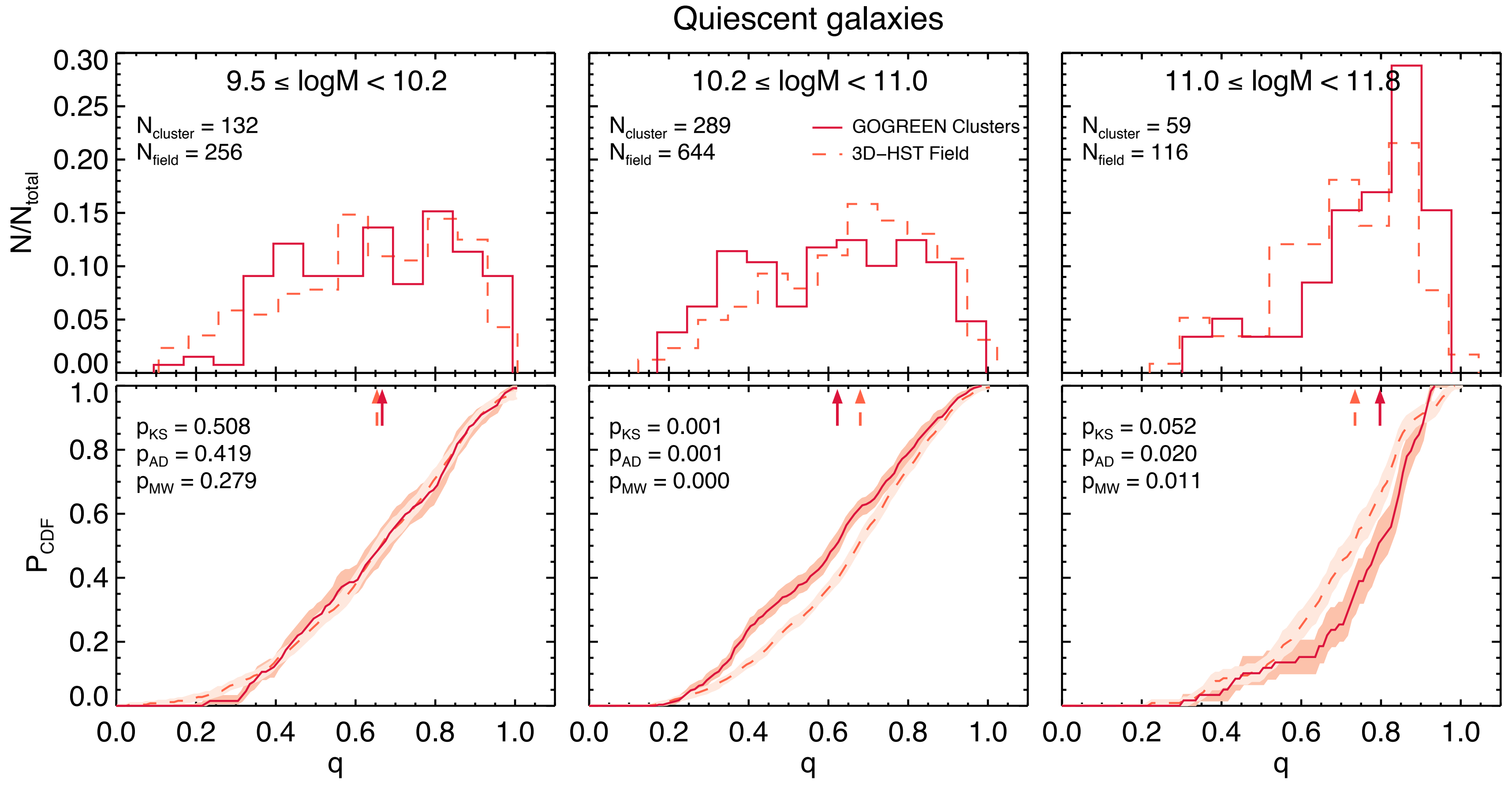

- Distribution of SF galaxies in cluster and the field are consistent with each other

- No obvious differences in the low-mass bin
- Cluster distribution in the middle mass bin shows broader q and a “dip” at q~0.5
- Cluster distribution at high mass show larger median q

Constraining the fraction of oblate ("disky") quiescent galaxies in cluster and field

- Projected axis ratio distributions can be used to reconstruct the intrinsic shapes of a galaxy population
- Studies show that axis ratio distributions of **local** ETGs can be accurately modeled by two-components:

- A **triaxial** set and an **oblate** set of galaxies with Gaussian distribution of intrinsic parameters
- The two-component model comprises 7 parameters – (T, σ_T, E, σ_E, b, σ_b, f_{ob})
  where T, E = triaxiallity and ellipticity of the triaxial set, b = intrinsic axis ratio of the oblate component
- **f_{ob}: the fraction of oblate galaxies in the population**

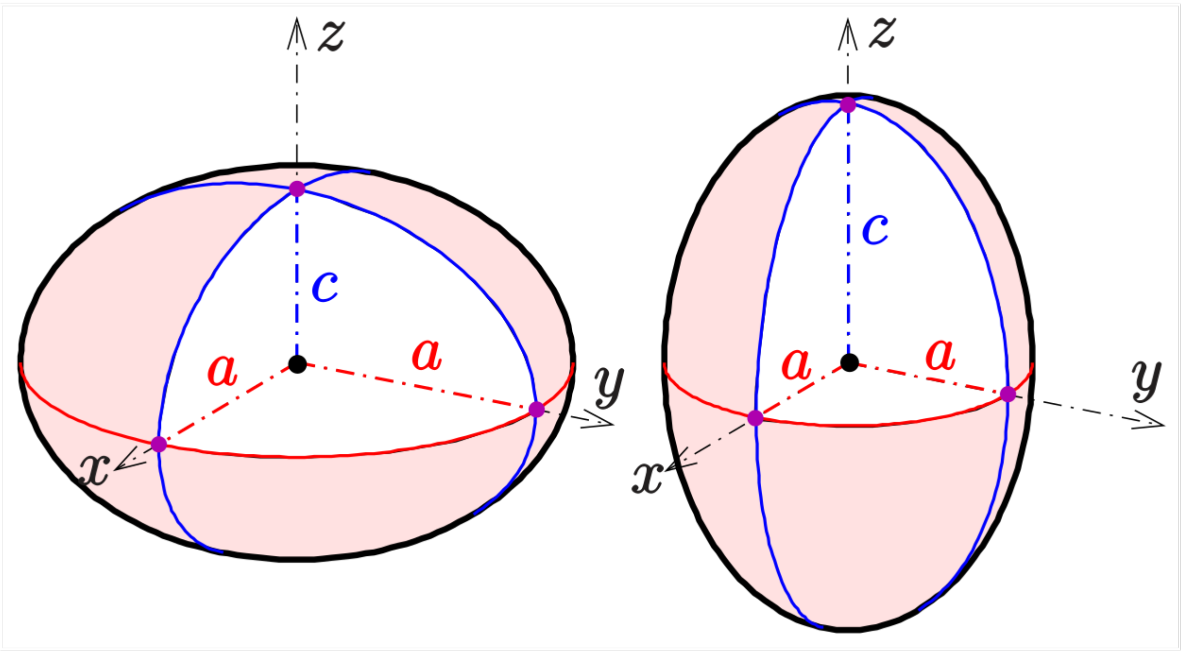

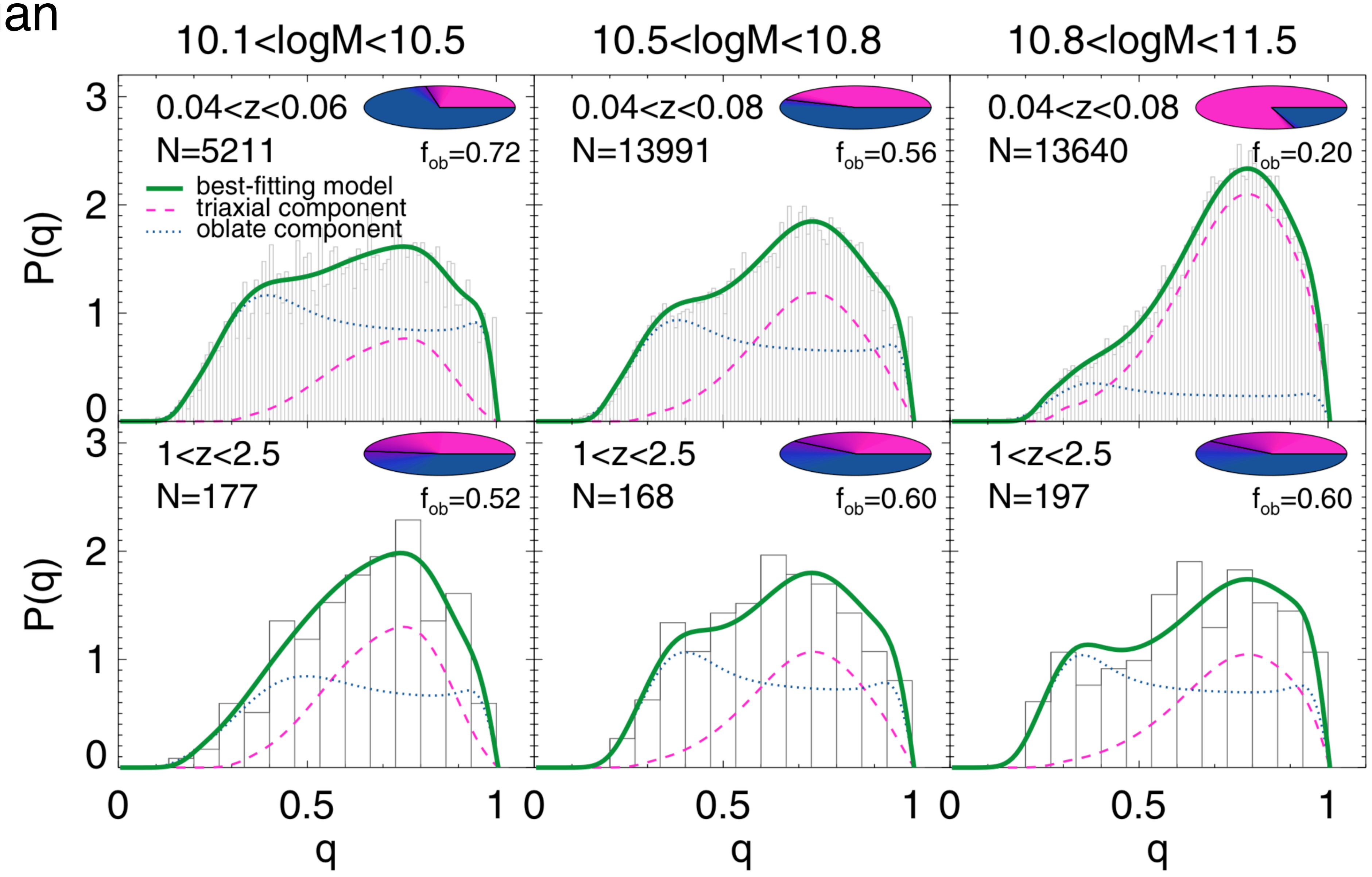

Chang+13 (see also Holden+12, van der Wel+14)

Constraining the fraction of oblate (“disky”) quiescent galaxies in cluster and field

- Projected axis ratio distributions can be used to reconstruct the intrinsic shapes of a galaxy population (Holden+12, Chang+13, van der Wel+14)

- A **triaxial** set and an **oblate** set of galaxies with Gaussian distribution of intrinsic parameters
- f_{ob}: the fraction of oblate galaxies in the population

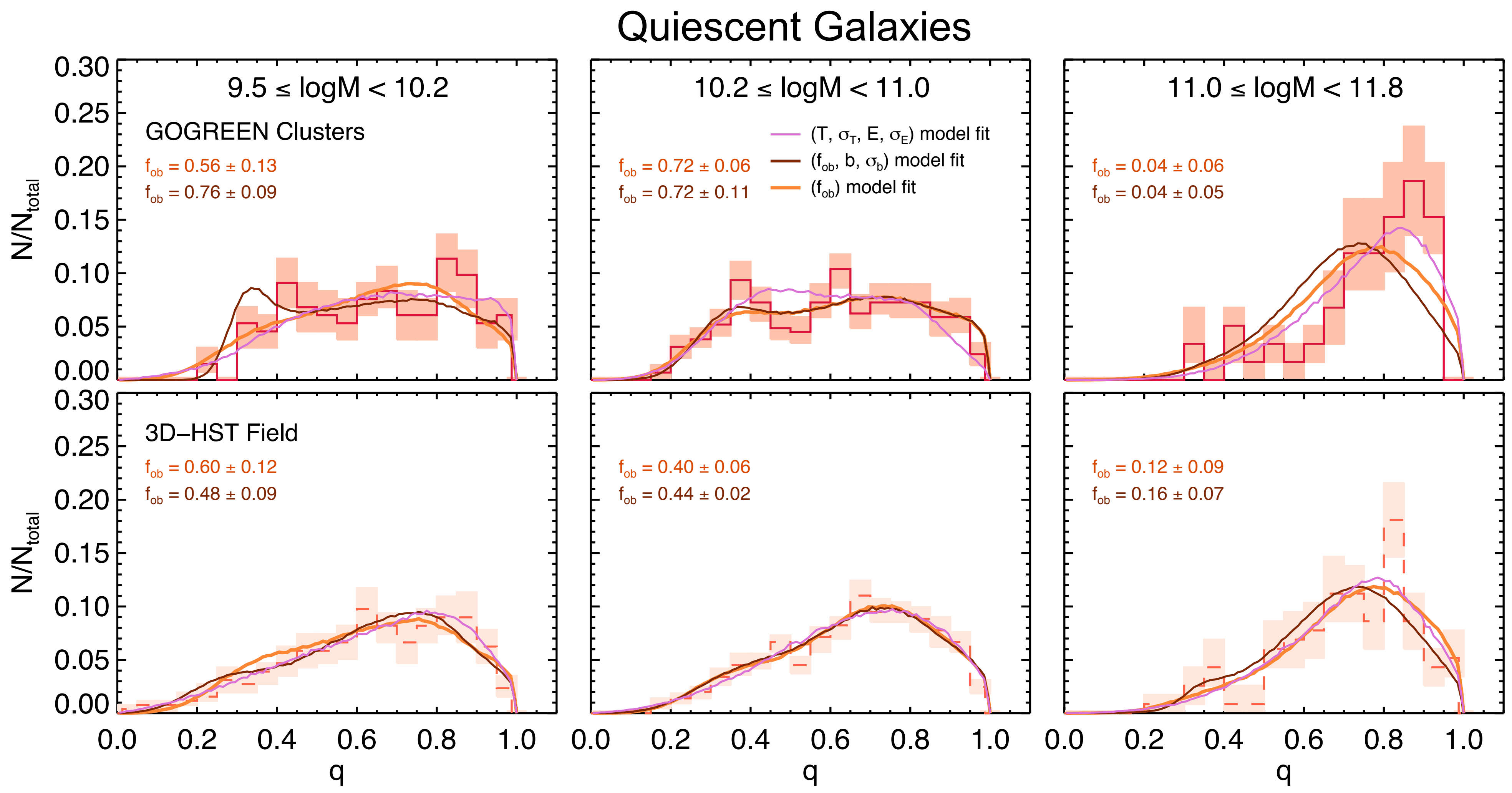

- **Middle mass bin** – Cluster have more disky galaxies than the field (f_{ob} = 0.72 vs 0.40)
- No evidence for a difference between the intrinsic shape of the oblate component (consistent *b*=0.29) in clusters and the field
- The single-component model cannot match the broad feature present in the cluster sample
- **High mass bin** – Massive galaxies in clusters intrinsically rounder (E=0.39 vs. 0.46)

Constraining the fraction of oblate ("disky") quiescent galaxies in cluster and field

- Projected axis ratio distributions can be used to reconstruct the intrinsic shapes of a galaxy population (Holden+12, Chang+13, van der Wel+14)

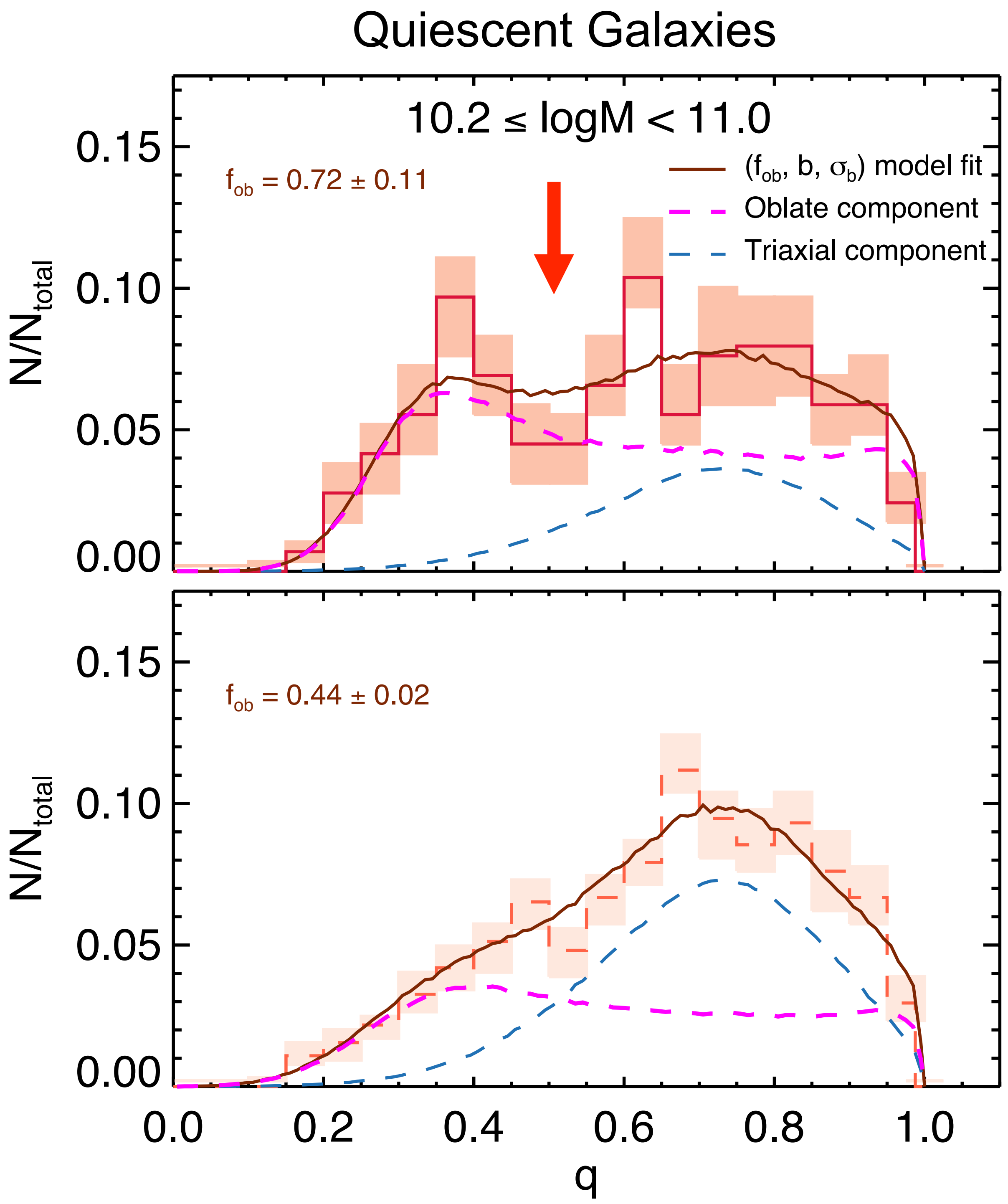

- **Middle mass bin** – Cluster have more disky galaxies than the field (f_{ob} = 0.72 vs 0.40)
- No evidence for a difference between the intrinsic shape of the oblate component (consistent *b*=0.29) in clusters and the field
- The single-component model cannot match the broad feature present in the cluster sample
- **High mass bin** – Massive galaxies in clusters intrinsically rounder (E=0.39 vs. 0.46)

Relation between environmental quenching and morphological transformation

- Combine the axis ratio results (middle mass) with the quenched fractions to study the excess quenching in the cluster sample to test the extent of morphological transformation:
- Cluster UVJ QF: **0.67**, Field QF: **0.28**
- Define $f_{QF} = (QF_{cluster} - QF_{field}) / QF_{cluster} \sim 0.6$, i.e. 60%

- Inject random SF galaxies from the field distribution into the Quiescent q field distribution until the resultant distribution has $f_{QF} * P_{SF}(q)$ (q from SF ~60%)

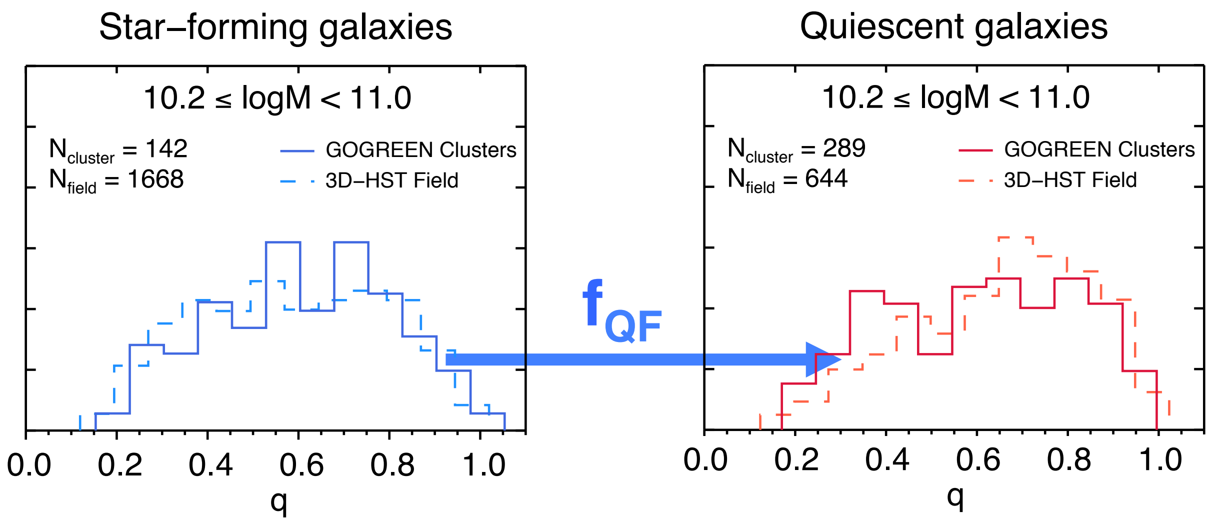

- The resultant toy model distribution is consistent with the observed distribution ($p_{KS} \sim 0.8$)
- ~60% of SF galaxies is, interestingly, the best match
- Consistent with no morphological transformation after being quenched

The resultant model (black)

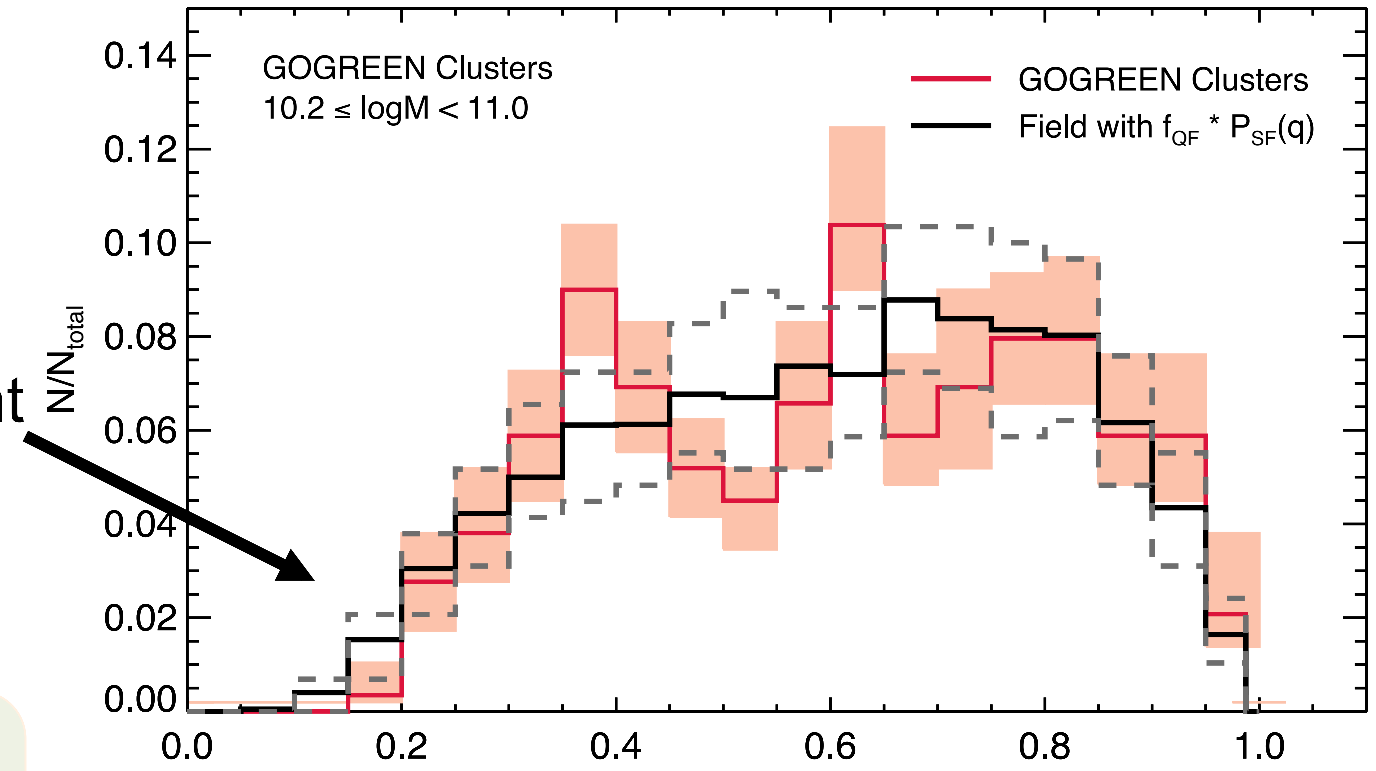

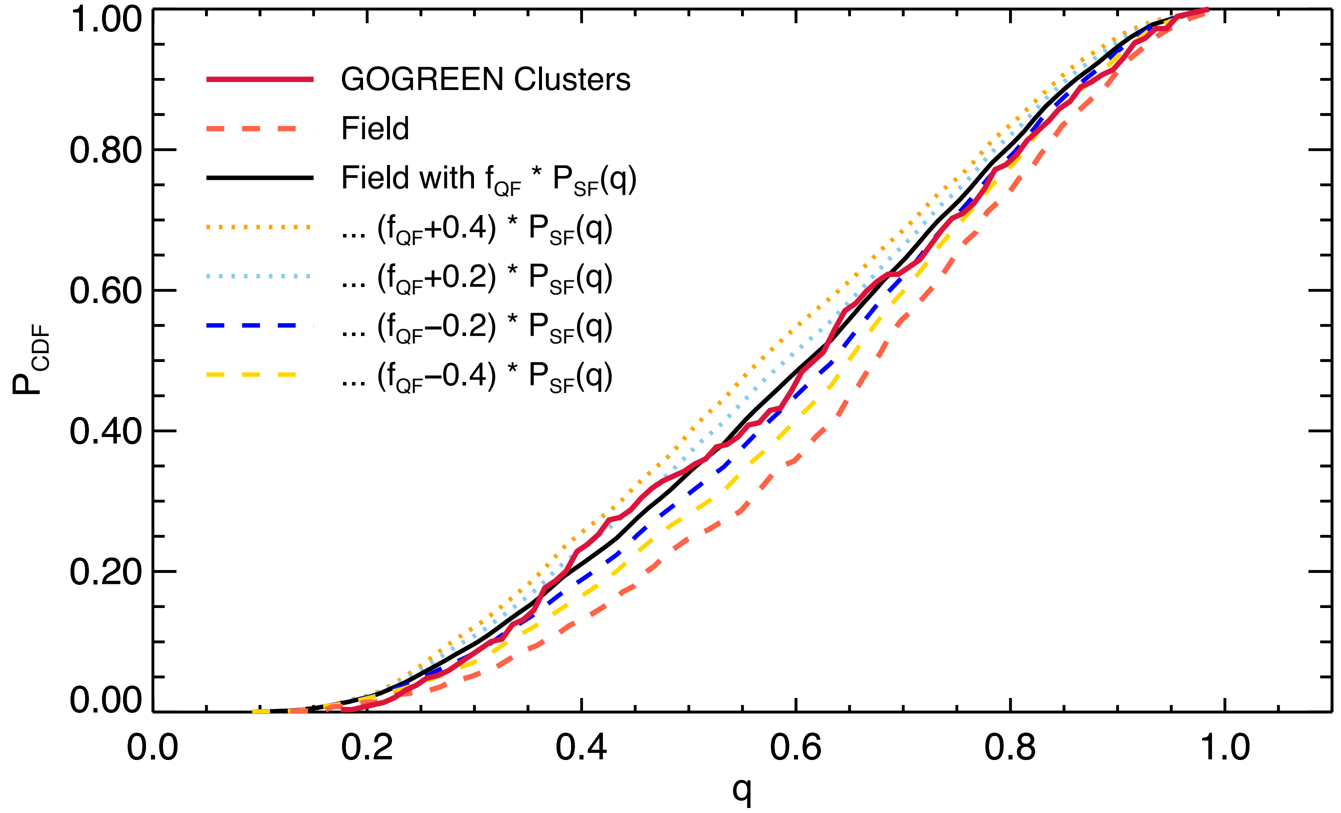

The age variation in the oblate quiescent population

- We utilize the mass-weighted age measurements from Webb+2020 to study the age variation with *q* in the quiescent population ($t_{univ,z} - t_{mw}$, i.e. the formation time, younger galaxies having a larger/later formation time)
- There are 163 quiescent galaxies that have both ages & *q* measurements

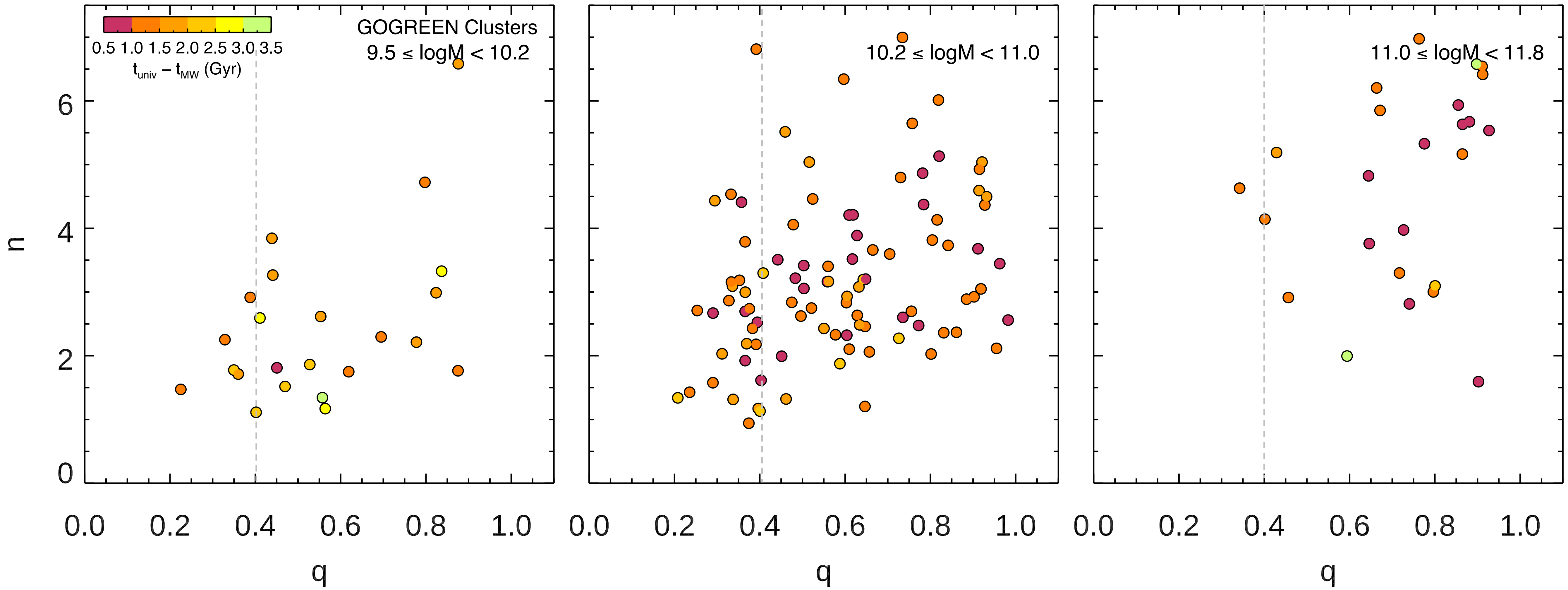

- The mass-weighted ages do not show a significant trend in *q*
- Not all disk-like galaxies in the cluster sample were recently quenched. Instead, some of them are formed and quenched early and stayed a disk until the epoch of observation.
- The age variation we see may imply that the quenching process that produces the disk excess has been occurring since high redshift.

Summary

- We compare the axis ratio distributions for 11 GOGREEN clusters at $1.0 < z < 1.4$ to a field sample to investigate the effect of the environment on galaxy structural properties.
- The median *q* of both star-forming galaxies and quiescent galaxies in clusters and the field increases with mass. Massive quiescent galaxies with $\log(M/M_{\odot}) \geq 11$ in both clusters and the field are on average rounder and and have a narrower *q* distribution than their low mass counterparts
- The *q* distribution of star-forming galaxies in clusters and field are consistent with each other
- The *q* distribution of quiescent galaxies in clusters and the field are distinct
- The difference between the cluster and the field sample in the intermediate mass range is consistent with the existence of an excess population of flattened, disk-like galaxies in clusters